The New Mechanistic Model to Illustrate the Complex Phenomena in Electrocoagulation Process of Vinasse

by Iqbal Syaichurrozi

Submission date: 05-Apr-2023 08:44AM (UTC+0700)
Submission ID: 2056159826
File name: e_Complex_Phenomena_in_Electrocoagulation_Process_of_Vinasse.pdf (4.46M)
Word count: 4909
Character count: 22803

Pol. J. Environ. Stud. Vol. 30, No. 4 (2021), 3249-3259
DOI: *10.15244/pjoes/130906* ONLINE PUBLICATION DATE: 2021-05-27

Original Research

The New Mechanistic Model to Illustrate the Complex Phenomena in Electrocoagulation Process of Vinasse

Iqbal Syaichurrozi[1,2], Sarto Sarto[1]*, Wahyudi Budi Sediawan[1], Muslikhin Hidayat[1]

[1]Department of Chemical Engineering, Faculty of Engineering, Universitas Gadjah Mada, Jl. Grafika No. 2, Yogyakarta 55281, Indonesia
[2]Department of Chemical Engineering, Faculty of Engineering, University of Sultan Ageng Tirtayasa, Jl. Jendral Soedirman Km 3, Cilegon 42435, Indonesia

Received: 4 October 2020
Accepted: 26 November 2020

Abstract

Electrocoagulation (EC) is one of potential methods in wastewater treatments. In treating vinasse waste through EC, complex phenomena occur during EC process. Hence, previous authors have developed mechanistic models, but the models have not illustrated the phenomena completely. Therefore, the goal of this study is to build the new model of EC and apply the model to simulate the EC phenomena in treating vinasse. Many parameters (current, pH, temperature, volume, anode weight loss, dissolved Fe concentration, chemical oxygen demand (COD) concentration, sludge mass and scum mass) are considered in developing this model. The adjustable kinetic constants in this model are k_{cg}, α, β, k_e, A_f, E_f. The results show that this model can fit the measured data of EC of vinasse at various voltages (7.5 and 12.5 V) with low Sum of Squares of Errors (SSE) value (0.0784-0.2758). The voltage of 12.5 V results higher k_{cg}, k_e, A_f and lower E_f values than 7.5 V.

Keywords: electrocoagulation, complex, mechanistic model, vinasse

Introduction

Electrocoagulation (EC) is one of treatment methods that are widely used to treat various wastewaters [1]. This method is successfully applied to remove organic pollutants. Compared with other methods, EC has many advantages because it needs low operating cost, produces hydrogen gas used as an alternative energy and results in sludge easily separated by sedimentation and flotation [2-7].

Basically, EC consists of three conventional methods i.e. electrolysis, coagulation and flotation. In electrolysis: oxidation process occurs at anode where anode (Fe) is dissolved to be Fe^{z+} ion and reduction process occurs at cathode where the H_2O is to be H_2 gas and OH^- ion [8]. In coagulation: chemical reaction between Fe^{z+} and OH^- resulted coagulant of $Fe(OH)_z$ adsorbing the pollutants to become the aggregates and then the sludge [4]. In flotation: the H_2 gas pushes the sludge on the surface as scum [9].

*e-mail: sarto@ugm.ac.id

For a better understanding of the EC process, currently, Syaichurrozi et al. [4] have proposed a mechanistic model of EC to illustrate the COD removal mechanism. The parameters included in the model are total COD concentration (g/L), remaining dissolved Fe concentration (g/L), sludge mass (g), scum mass (g) and current value (A). In the model, the working volume is assumed to be constant and changes of temperature and pH during process are not considered. The model is successfully applied to simulate the measured data from EC process at voltage of 10 V with retention time of 1 h. Furthermore, at higher voltage, the working volume decreases drastically, so it is not constant. Thus, Syaichurrozi et al. [9] have built new models to consider the change of the working volume. Besides that, they have proposed four routes for organic pollutant (expressed as chemical oxygen demand (COD)) using four mechanistic models. The results show that, the Electrocoagulation Mechanistic Model No. 2 (EMM2) results in the most precision all of the proposed models. The important points obtained by the EMM2 are that the volume is not constant, the sludge is formed by reaction between Fe and COD and then the scum is resulted by degradation of sludge. However, the EMM2 did not consider the change of pH and temperature during process. Factually, pH and temperature of solution increases during EC. Therefore, the new mechanistic model needs to be developed to simulate the complex process of EC.

The complex phenomena in EC appear when it is applied to treat waste having very high organic pollutant such as vinasse. It is a waste resulted from distillation unit as bottom product. It contains very high organic pollutant (COD) and low pH value. Some authors have reported studies about EC of vinasse [10-14]. The origin vinasse in the study of Yavuz [10] and Khandegar and Saroha [11] contains COD concentration of 4,750 and 3,360 mg/L respectively. Meanwhile, it in the study of Aziz et al. [14] contains COD concentration of 8,500 mg/L but in their experiment, it has been diluted to be 2,000 mg/L. The extreme dilution occurred in study of Asaithambi et al. [12-13] in which the vinasse has been diluted from 80,000-90,000 to become 2,500 mg/L. The dilution way is not suggested because it will make the total volume of the waste to be very much more.

In this study, the Indonesian vinasse contains very high COD concentration (more than 100,000 mg/L). This waste is very dangerous if it discharged to the water body without treatment. Currently, the focus of this study is development of the new mechanistic model and validation of the model with experimental data of EC of vinasse at various voltages obtained from a previous study [9].

Methods

Development of Kinetic Model

Anode Weight Loss

The first reaction in EC is electrolysis. In this reaction, anode experiences oxidation, so it is sacrificed to result Fe^{z+} (Eq. 1). Meanwhile, reduction occurs in cathode in which the water is converted to OH^- ion and H_2 gas (Eq. 2) [15]. The rate of anode weight loss could be estimated based on Faraday's law (Eq. 3) [4]. The z value can be 2 or 3 but the appropriate z value is 2. It means that ferrous (Fe^{2+}) is a product of oxidation when iron is used as anode [4, 9].

$$Fe \xrightarrow{\text{oxidation}} Fe^{2+} + 2\,e^- \quad (1)$$

$$2\,H_2O + 2\,e^- \xrightarrow{\text{reduction}} H_2 + 2\,OH^- \quad (2)$$

$$\frac{dm_{anode}}{dt} = -\frac{IBM_{Fe}}{zF} = -\frac{JA_eBM_{Fe}}{zF} \quad (3)$$

Net Rate of Dissolved Fe Mol Production

Based on Eq. 1, oxidation occurs in anode and the product of the reaction is Fe^{2+}. Furthermore, the Fe^{2+} will undergo hydrolysis reaction to be $Fe(OH)^+$, $Fe(OH)_2^0$, $Fe(OH)_{2(s)}$, $Fe(OH)_3^-$ [8]. Therefore, for simplification of the model, in assumption, there are only the two species exist in the solution which are Fe^{2+} and $Fe(OH)_{2(s)}$. Equilibrium between the two iron species is shown in Eq. 4.

$$Fe(OH)_2 \overset{K_s}{\leftrightarrow} Fe^{2+} + 2\,OH^- \quad (4)$$

The solubility of $Fe(OH)_2$ (based on Eq. 4) is expressed by Eq. 5.

$$K_s = [Fe^{2+}][OH^-]^2 \quad (5)$$

Because of $[OH^-] = \frac{K_w}{[H^+]} = K_w 10^{pH}$, Eq. 5 is rearranged to Eq. 6.

$$K_s = [Fe^{2+}]{K_w}^2 10^{2pH} \quad (6)$$

$$[Fe^{2+}] = [Fe]_{sat} = \frac{K_s}{{K_w}^2 10^{2pH}} \quad (7)$$

$$nFe_{sat} = \frac{K_s}{{K_w}^2 10^{2pH}} v \quad (8)$$

Production of dissolved Fe mol by electrodissolution in anode during EC could be predicted by Faraday's law (Eq. 9).

$$\frac{dnFe_d}{dt} = \frac{I}{zF} = \frac{JA_e}{zF} \quad (9)$$

Furthermore, after saturation, $Fe(OH)_{2(s)}$ is formed and acts as coagulant to remove pollutant to make sludge. The production rate of $Fe(OH)_{2(s)}$ mol is predicted by Eq. 10 (adapted from [16]).

$$\frac{dnFe(OH)_2}{dt} = k_{cg}(nFe_d - nFe_{sat})$$
$$\frac{dnFe(OH)_2}{dt} = k_{cg}\left(nFe_d - \frac{K_s}{K_w{}^2 10^{2pH}} v\right) \quad (10)$$

Therefore, the net rate of Fe^{2+} mol production could be written through Eq. 11.

$$\frac{dnFe_d}{dt} = \underbrace{\frac{JA_e}{zF}}_{electrodissolution} \underbrace{- k_{cg}\left(nFe_d - \frac{K_s}{K_w{}^2 10^{2pH}} v\right)}_{coagulation\ formation} \quad (11)$$

Because of inconstant working volume during EC, the Eq. 11 is modified to Eq. 12.

$$\frac{d([Fe]_d v)}{dt} = \frac{JA_e}{zF} - k_{cg}\left(nFe_d - \frac{K_s}{K_w{}^2 10^{2pH}} v\right)$$
$$[Fe]_d \frac{dv}{dt} + v\frac{d[Fe]_d}{dt} = \frac{JA_e}{zF} - k_{cg}\left([Fe]_d v - \frac{K_s}{K_w{}^2 10^{2pH}} v\right)$$
$$[Fe]_d v' + v\frac{d[Fe]_d}{dt} = \frac{JA_e}{zF} - k_{cg}\left([Fe]_d - \frac{K_s}{K_w{}^2 10^{2pH}}\right) v$$
$$\frac{d[Fe]_d}{dt} = \frac{\frac{JA_e}{zF} - k_{cg}\left([Fe]_d - \frac{K_s}{K_w{}^2 10^{2pH}}\right)v - [Fe]_d v'}{v} \quad (12)$$

Net Rate of $Fe(OH)_2$ Mass Production

The production rate of $Fe(OH)_2$ mol is shown in Eq. 10. Furthermore, it is rearranged in mass unit (Eq. 13).

$$\frac{dmFe(OH)_2}{dt} = BM_{Fe(OH)_2} k_{cg}\left([Fe]_d - \frac{K_s}{K_w{}^2 10^{2pH}}\right) v \quad (13)$$

Furthermore, the coagulant will adsorb the COD to make sludge [4, 9]. The adsorption reaction is assumed as Eq. 14.

$$Fe(OH)_2 + COD \xrightarrow{k_a} 2\ Sludge \quad (14)$$

This model assumes that adsorption reaction occurs between coagulant and COD in mass unit, not in mol unit. Based on Eq. 14, the consumption rate of coagulant mass could be written by Eq. 15.

$$\frac{dmFe(OH)_2}{dt} = -k_a C_{Fe(OH)_2} C_{COD} v \quad (15)$$

Therefore, the net rate of coagulant mass production is written by Eq. 16.

$$\frac{dmFe(OH)_2}{dt} = BM_{Fe(OH)_2} k_{cg}\left([Fe]_d - \frac{K_s}{K_w{}^2 10^{2pH}}\right) v - k_a C_{Fe(OH)_2} C_{COD} v \quad (16)$$

In assumption, the coagulant (precipitate of $Fe(OH)_2$) does not remain in solution because it is to become sludge and scum completely, so $\frac{dmFe(OH)_2}{dt} = 0$.

$$0 = BM_{Fe(OH)_2} k_{cg}\left([Fe]_d - \frac{K_s}{K_w{}^2 10^{2pH}}\right) v - k_a C_{Fe(OH)_2} C_{COD} v$$
$$k_a C_{Fe(OH)_2} C_{COD} v = BM_{Fe(OH)_2} k_{cg}\left([Fe]_d - \frac{K_s}{K_w{}^2 10^{2pH}}\right) v$$
$$C_{Fe(OH)_2} = \frac{BM_{Fe(OH)_2} k_{cg}\left([Fe]_d - \frac{K_s}{K_w{}^2 10^{2pH}}\right) v}{k_a C_{COD} v} \quad (17)$$

Net Rate of COD Mass Consumption

Based on Eq. 14, the consumption rate of COD mass could be written by Eq. 18.

$$\frac{dmCOD}{dt} = -k_a C_{Fe(OH)_2} C_{COD} v \quad (18)$$

Entrapment reaction also occurs in sludge formation [4, 9]. Thus, Eq. 18 is extended to Eq. 19.

$$\frac{dmCOD}{dt} = \underbrace{-k_a C_{Fe(OH)_2} C_{COD} v}_{adsorption} - \underbrace{k_e C_{COD} v}_{entrapment} \quad (19)$$

Substitute Eq. 17 to Eq. 19 to build Eq. 20.

$$\frac{dmCOD}{dt} = -k_a \frac{BM_{Fe(OH)_2} k_{cg}\left([Fe]_d - \frac{K_s}{K_w{}^2 10^{2pH}}\right) v}{k_a C_{COD} v} C_{COD} v - k_e C_{COD} v$$
$$\frac{dmCOD}{dt} = -BM_{Fe(OH)_2} k_{cg}\left([Fe]_d - \frac{K_s}{K_w{}^2 10^{2pH}}\right) v - k_e C_{COD} v \quad (20)$$

Because of inconstant working volume, Eq. 20 is rearranged to Eq. 21.

$$\frac{d(C_{COD} v)}{dt} = -BM_{Fe(OH)_2} k_{cg}\left([Fe]_d - \frac{K_s}{K_w{}^2 10^{2pH}}\right) v - k_e C_{COD} v$$
$$C_{COD}\frac{dv}{dt} + v\frac{dC_{COD}}{dt} = -BM_{Fe(OH)_2} k_{cg}\left([Fe]_d - \frac{K_s}{K_w{}^2 10^{2pH}}\right) v - k_e C_{COD} v$$
$$\frac{dC_{COD}}{dt} = \frac{-BM_{Fe(OH)_2} k_{cg}\left([Fe]_d - \frac{K_s}{K_w{}^2 10^{2pH}}\right) v - k_e C_{COD} v - C_{COD} v'}{v} \quad (21)$$

Net Rate of Sludge Mass Production

The sludge mass is resulted from reactions of adsorption and entrapment. Meanwhile, the sludge mass consumption rate is caused by scum formation (Eq. 22)

[4, 9]. Therefore, the net rate of sludge mass production is expressed by Eq. 23.

$$\text{Sludge} \xrightarrow{k_f} \text{Scum} \tag{22}$$

$$\frac{dm_{sludge}}{dt} = 2BM_{Fe(OH)_2}k_{cg}\left([Fe]_d - \frac{K_s}{{K_w}^2 10^{2pH}}\right)v + k_e C_{COD} v - \underbrace{k_f m_{sludge}}_{flotation} \tag{23}$$

Net Rate of Scum Mass Production

Based on Eq. 22, the scum is formed by flotation. Therefore, the net rate of scum mass production is expressed by Eq. 24.

$$\frac{dm_{scum}}{dt} = k_f m_{sludge} \tag{24}$$

Mechanistic Model with Temperature Dependence

For assumption of no temperature dependence, the mathematic equations included in the model are Eqs. 3, 12, 21, 23, 24. However, in the fact, solution temperature changes as function of time. Therefore, mathematic equations (in Eqs 3, 12, 21, 23, 24) have to be modified by considering the temperature change during EC process. The kinetic constants are k_{cg}, K_s, K_w, k_e and k_f. Chemical process is much more affected by temperature than physical process. The kinetic constants contributing in chemical processes are K_s, K_w and k_f and those in physical processes are k_{cg} and k_e. Hence, the K_s, K_w and k_f are modified with consideration of temperatur change and k_{cg} and k_e are assumed not affected by temperature change.

The equilibrium constants (K_s and K_w) are modified through Van't Hoff equation. The Van't Hoff equation as function of temperature for K_s is shown by Eq. 25 [17].

$$ln\frac{K_s}{K_{s0}} = \frac{-\Delta H_s}{R}\left(\frac{1}{T} - \frac{1}{T_0}\right) \tag{25}$$

Furthermore, Eq. 25 is rearranged to Eq. 26.

$$ln\frac{K_s}{K_{s0}} = \frac{\Delta H_s}{RT_0} - \frac{\Delta H_s}{RT}$$
$$\frac{K_s}{K_{s0}} = exp\left(\frac{\Delta H_s}{RT_0}\right) exp\left(-\frac{\Delta H_s}{RT}\right)$$
$$K_s = K_{s0}\, exp\left(\frac{\Delta H_s}{RT_0}\right) exp\left(-\frac{\Delta H_s}{RT}\right) \tag{26}$$

Assuming that $K_{s0} exp\left(\frac{\Delta H_s}{RT_0}\right) = K_{s0}'$, so Eq. 26 is modified to Eq. 27.

$$K_s = K_{s0}'\, exp\left(-\frac{\Delta H_s}{RT}\right) \tag{27}$$

By the same way with K_s, the K_w is modified to Eq. 28.

$$K_w = K_{w0}'\, exp\left(-\frac{\Delta H_w}{RT}\right) \tag{28}$$

Therefore,

$$\frac{K_s}{{K_w}^2} = \frac{K_{s0}'\, exp\left(-\frac{\Delta H_s}{RT}\right)}{\left(K_{w0}'\, exp\left(-\frac{\Delta H_w}{RT}\right)\right)^2} = \frac{K_{s0}'}{(K_{w0}')^2} exp\left(\frac{-\Delta H_s - 2(-\Delta H_w)}{RT}\right)$$
$$\frac{K_s}{{K_w}^2} = \alpha \exp\left(\frac{\beta}{RT}\right) \tag{29}$$

with:

$$\alpha = \frac{K_{s0}'}{(K_{w0}')^2} \tag{30}$$

$$\beta = -\Delta H_s - 2(-\Delta H_w) \tag{31}$$

Furthermore, the k_f is modified through Arrhenius equation (Eq. 32) [18].

$$k_f = A_f \exp\left(-\frac{E_f}{RT}\right) \tag{32}$$

Substitution Eqs 29 and 32 to Eqs 3, 12, 21, 23 and 24 to get new mathematical equations and then shown in Table 1.

The summary of the final mathematic equations is shown in Table 1. The change of current density, pH and temperature profile is approached by using an empirical curve (see section 5.1). The change of working volume during EC is identified by the change of vinasse surface (x) in reactor. Also, the value of x is approached by using an empirical curve (see section 5.1). Furthermore, the values of A_e, v and v' is calculated by using formulas shown in Table 1 [9].

Simulation

The adjustable kinetic constants in this model are k_{cg}, α, β, k_e, A_f, E_f. The values of the constants are obtained by minimization of SSE (Sum of Squared Error) (Eq. 33). The model (simultaneous ordinary differential equations, Table 1) is solved using MATLAB program with ode15s solver and minimizing SSE with fminsearch [9].

Sum of Squares of Errors (SSE)

$$= \sum_{i=1}^{n}\left(\frac{measureddata - predicteddata}{measureddata}\right)^2 \tag{33}$$

Experimental Data

The experimental data used to validate the model are obtained from a previous study [9]. The data is obtained from EC experiment using a lab-scale-batch

Table 1. Summary of mathematic equations for the mechanistic model with temperature dependence.

Rate	Mathematic Equation
$\frac{dm_{anode}}{dt}$	$-\frac{JA_eBM_{Fe}}{zF}$
$\frac{d[Fe]_d}{dt}$	$\frac{\frac{JA_e}{zF} - k_{cg}\left([Fe]_d - \frac{\alpha \exp\left(\frac{\beta}{RT}\right)}{10^{2pH}}\right)v \ - [Fe]_d v'}{v}$
$\frac{dC_{COD}}{dt}$	$\frac{-BM_{Fe(OH)2}k_{cg}\left([Fe]_d - \frac{\alpha \exp\left(\frac{\beta}{RT}\right)}{10^{2pH}}\right)v - k_eC_{COD}v - C_{COD}v'}{v}$
$\frac{dm_{sludge}}{dt}$	$2BM_{Fe(OH)2}k_{cg}\left([Fe]_d - \frac{\alpha \exp\left(\frac{\beta}{RT}\right)}{10^{2pH}}\right)v + k_eC_{COD}v - A_f \exp\left(-\frac{E_f}{RT}\right)m_{sludge}$
$\frac{dm_{scum}}{dt}$	$A_f \exp\left(-\frac{E_f}{RT}\right)m_{sludge}$
J, pH, T, x	*f(t)*
A_e	$2(l_e - x)w_e + 2(l_e - x)t_e + w_e t_e$
v	$v_0 - A_R x$
v'	$\frac{dv}{dt}$

reactor with cylindrical shape having diameter 1.1 dm and height of 1.55 dm. Iron is used as anode and cathode with active dimension of length, width, thickness of 0.95, 0.3, 0.03 dm respectively. The value of inter-electrode is maintained to be constant in 0.55 dm. The voltage is varied to be 7.5 V and 12.5 V. The measured parameters were total COD concentration (g/dm^3), remaining dissolved Fe (g/dm^3), sludge mass (g), scum mass (g), current (A), *x* (dm), temperature (K), anode weight (g). The complete data is shown in Table 2. Because the unit of dissolved Fe in the model is mol/dm^3, the dissolved Fe (g/dm^3) in Table 2 is converted to unit of mol/dm^3 by divided it with BM of Fe (56 g/mol).

Results and Discussions

Empirical Equation for pH, T, *x*, J

The solution pH changes during EC process (Table 2) because of OH^- accumulation in solution. It is resulted from reduction at cathode (Eq.2). The pH solution in vinasse increases faster at voltage of 12.5 V than at 7.5 V because the current value at the former is higher than that at the later (Table 2). The mol amount of OH^- ion is directly proportional with current value. From Fig. 1a), mathematic equations between pH and electrolysis time at 7.5 and 12.5 V are obtained as:

$$pH_{7.5V} = 8 \times 10^{-8}\, t^2 + 5 \times 10^{-5}\, t + 6.004 \ (R^2 = 0.988) \quad (34)$$

$$pH_{12.5V} = -2 \times 10^{-7}\, t^2 + 1 \times 10^{-3}\, t + 5.811 \ (R^2 = 0.932) \quad (35)$$

Similar with solution pH, the solution temperature increases until the end of process. It has a correlation with current. The energy supplied from electrolysis can be estimated using formula in Eq.36. Furthermore, the energy received by the solution can be estimated using Eq. 37.

$$Q = VIt \quad (36)$$

$$Q = C_p \Delta T \quad (37)$$

Clearly, the increase in temperature is caused by supply of current continuously in solution during process. From Fig. 1b), mathematic equations between temperature and electrolysis time at 7.5 and 12.5 V are obtained as:

Table 2. Experimental data during EC of vinasse waste at various voltages [9].

7.5 V										
t (s)	I (A)	T (K)	pH	*x* (dm)	Scum (g)	COD (g/dm³)	Dissolved Fe (g/dm³)	Dissolved Fe (mol/dm³)	Anode weight loss (g)	J (A/dm²)
0	2.15	302.65	6.0	0.000	0.00	100.16	0.039	0.000693	0	3.38
600	2.16	304.15	6.1	0.020	0.28	97.36	Na	Na	Na	3.47
1200	2.20	306.65	6.1	0.045	1.42	92.87	0.398	0.007112	Na	3.63
1800	2.22	307.35	6.4	0.065	2.78	92.65	Na	Na	Na	3.74
2400	2.18	308.65	6.6	0.085	4.05	92.65	0.923	0.016483	Na	3.76
3000	2.10	309.65	6.8	0.105	5.30	91.08	Na	Na	Na	3.71
3600	2.05	310.15	7.2	0.125	6.90	91.08	0.886	0.015817	-2.241	3.70
12.5 V										
t (s)	I (A)	T (K)	pH	*x* (dm)	Scum (g)	COD (g/dm³)	Dissolved Fe (g/dm³)	Dissolved Fe (mol/dm³)	Anode weight loss (g)	J (A/dm²)
0	3.76	302.15	6.0	0.000	0.00	100.16	0.039	0.000693	0	5.91
600	4.17	308.65	6.3	0.090	1.54	95.79	Na	Na	Na	7.23
1200	4.25	314.65	6.8	0.160	5.32	92.65	0.560	0.009997	Na	8.01
1800	4.26	319.85	7.5	0.215	9.47	91.08	Na	Na	Na	8.62
2400	4.08	324.35	7.7	0.275	14.44	87.94	0.529	0.009447	Na	8.98
3000	3.88	328.15	7.7	0.375	19.35	84.80	Na	Na	Na	9.99
3600	3.53	330.65	7.3	0.440	26.78	83.17	0.490	0.008748	-4.328	10.21

$$T_{7.5V} = -4 \times 10^{-7}\, t^2 + 3 \times 10^{-3}\, t + 302.5 \quad (R^2 = 0.991) \tag{38}$$

$$T_{12.5V} = -1 \times 10^{-6}\, t^2 + 1.1 \times 10^{-2}\, t + 302 \quad (R^2 = 0.999) \tag{39}$$

The surface of vinasse in reactor decreases because reduction reaction of water, evaporation of water and scum formation [9]. Fig. 1c) shows the mathematic equation between *x* and electrolysis time with detailed equations for 7.5 and 12.5 V as:

$$x_{7.5V} = 3.51 \times 10^{-5}\, t \quad (R^2 = 0.998) \tag{40}$$

$$x_{12.5V} = 12.21 \times 10^{-5}\, t \quad (R^2 = 0.993) \tag{41}$$

Furthermore, current density profile during process is function electrolysis time shown by Fig. 1d) with detailed equations as:

$$J_{7.5V} = -6 \times 10^{-8}\, t^2 + 2.9 \times 10^{-4}\, t + 3.356 \quad (R^2 = 0.958) \tag{42}$$

$$J_{12.5V} = -2 \times 10^{-7}\, t^2 + 1.72 \times 10^{-3}\, t + 6.058 \quad (R^2 = 0.985) \tag{43}$$

All the empirical equations (Eqs 34-35 and 38-43) are used in the mechanistic model having mathematic equations shown on Table 1. The equations show that complex phenomena occur during EC process because pH, T, *x* and J change as function of time. Furthermore, the changes of anode weight, COD concentration, dissolved Fe concentration, scum mass and sludge mass are predicted using the mechanistic model and the results are discussed in section 5.2.

Application of the New Model

The new mechanistic model successfully simulates the behavior of COD removal during EC of vinasse with very low SSE value (0.0784-0.2758, Table 3). The visualization between experiment and predicted data is depicted in Fig. 2(a-e). Also, the kinetic constants are shown in Table 3 in detail.

Anode Weight Loss and Dissolved Fe

Anode weight loss is successfully predicted by Faraday's law with z = 2 (Fig. 2a). This value confirms that the product of oxidation is Fe^{2+}. Furthermore, Fig. 2b) shows the remaining dissolved Fe in solution. It in vinasse during EC at 12.5 V is less than at 7.5 V. It is related to solution pH where the higher the pH, the low solubility of Fe. Hence, the solubility of Fe at

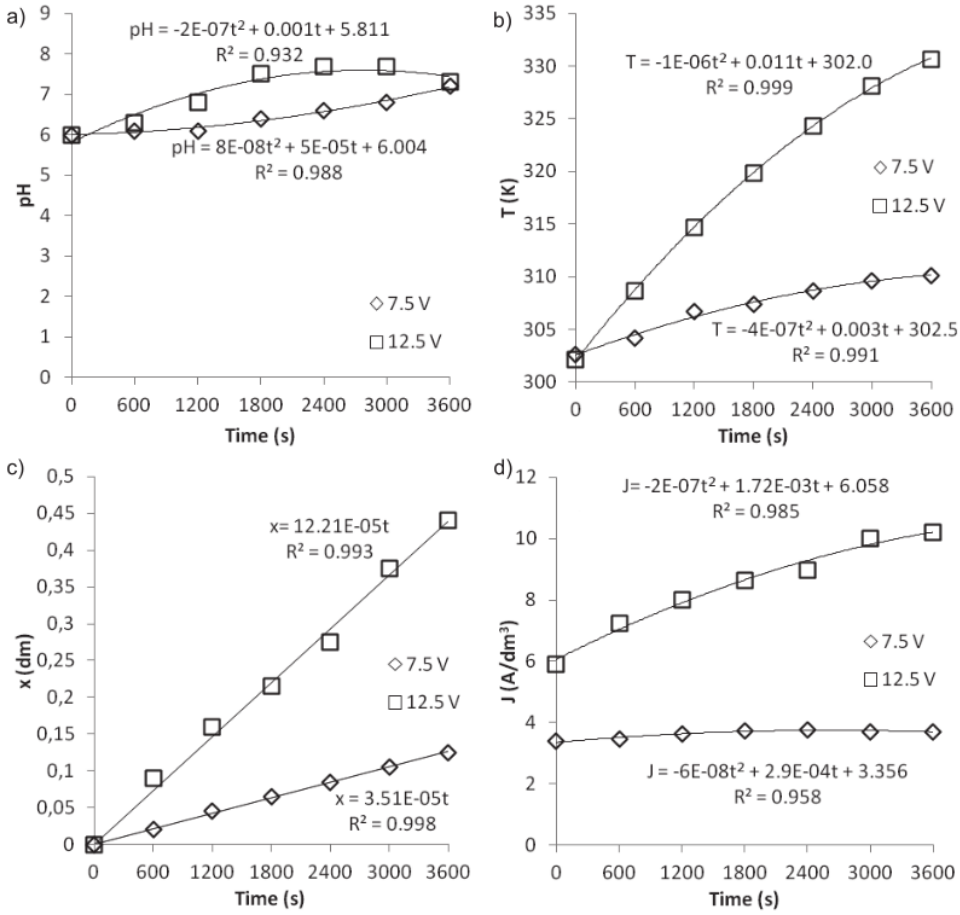

Fig. 1. The empirical equation for changes of a) solution pH, b) solution temperature, c) surface vinasse in reactor and d) current density

12.5 V is lower than at 7.5 V because the former increases the pH more rapidly. The solubility is also affected by solution temperature. In theory, higher temperature will result higher solubility. In the fact, voltage of 12.5 V results lower solubility of Fe although it results solution temperature higher than 7.5 V. Hence, the solubility of Fe in vinasse is mainly affected by pH, not temperature.

The k_{cg} presents the rate of coagulant formation. This kinetic constant is affected by the solubility of Fe and current value. The current value at 12.5 V is higher than that at 7.5 V (Table 2). The higher the current value, the more the Fe^{2+} mol is resulted from oxidation reaction. Hence, total Fe^{2+} mol at 12.5 V is higher than that at 7.5 V. Meanwhile, the solubility of Fe at 12.5 V is lower, so much more coagulant is formed at this voltage than the lower voltage. The k_{cg} in 12.5 V (3.20×10^{-3} /s) is higher than that in 7.5 V (8.06×10^{-4} /s).

The constants of α and β for 7.5 V is almost same with those for 12.5 V. This shows that enthalpy process is not affected significantly by temperature change. This is in line with Van't Hoff assumption in which the enthalpy process is no temperature dependence.

COD Concentration

The profile of decrease in COD concentration is also successfully predicted by the new model (Fig. 2c). Based on explanation in section 5.2.1, voltage of 12.5 V results more coagulant than 7.5 V, so the former can remove the COD in larger amount than the later. Furthermore 12.5 V also results higher k_e value than 7.5 V. It means, the entrapment reaction is easier to hold when the coagulant is resulted in larger amount.

Sludge and Scum Mass

The evolution of sludge and scum mass during EC is predicted and shown in Fig. 2(d,e). Voltage of 12.5 V results more sludge and scum mass than 7.5 V.

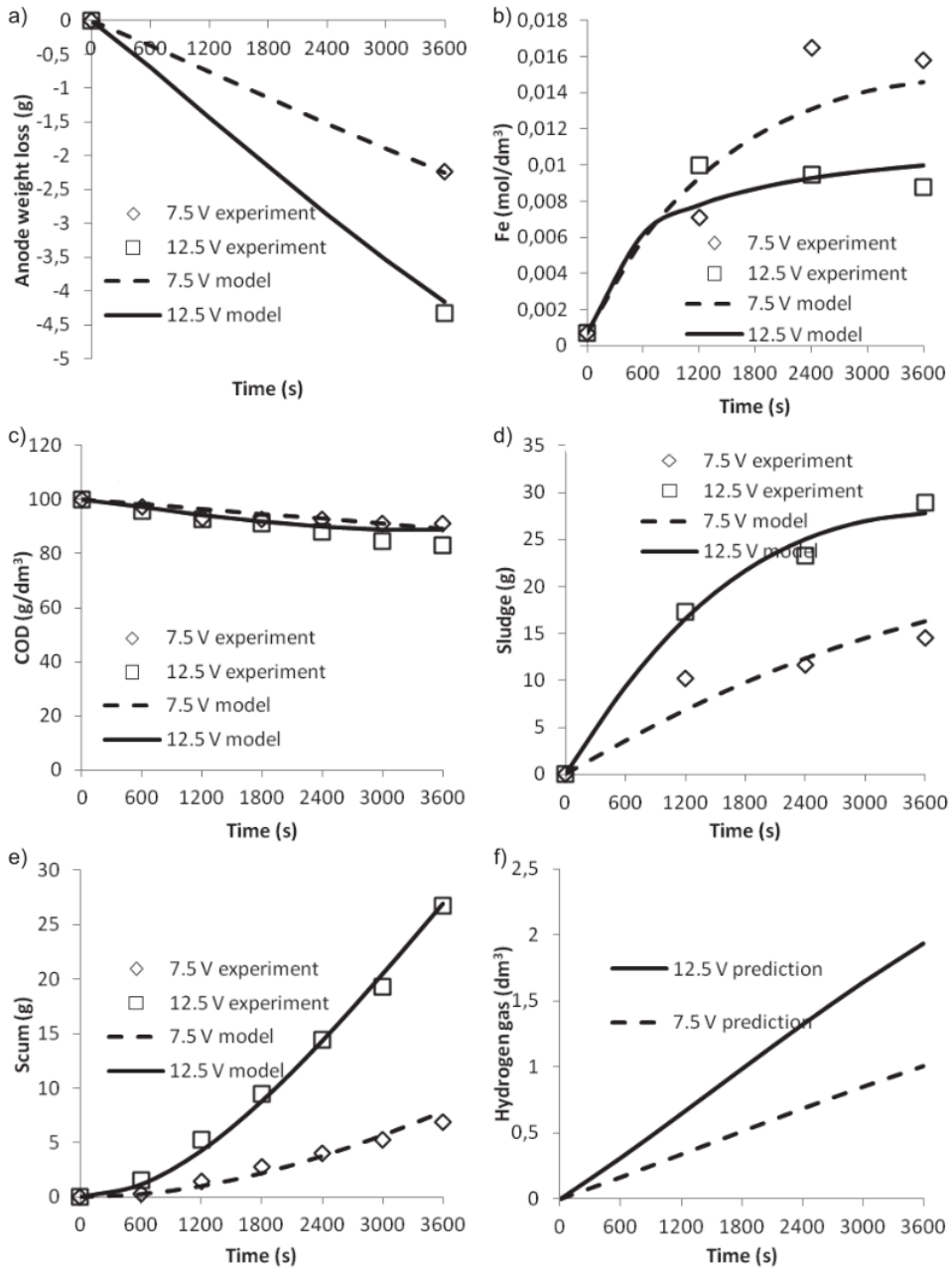

Fig. 2. Fitting between experimental and predicted data from the new kinetic model for a) anode weight loss, b) concentration of Fe, c) concentration of COD, d) mass of sludge, e) mass of scum; and then f) prediction of Hydrogen gas based on Faraday's Law.

The sludge is formed from adsorption of COD on coagulant and settles on the bottom of EC reactor. Furthermore the sludge is broken and goes to surface of vinasse as scum by evolution of H_2. The production of H_2 in mol unit could be predicted through Faraday's law showed in Eq. 44 [9]. The unit of H_2 could be converted in L unit by using Eq. 45.

$$\frac{dn_{H_2}}{dt} = \frac{I}{F}H = \frac{JA_e}{F}H = \frac{JA_e}{F}H \quad (44)$$

Table 3. Kinetic constant values in simulation of the experimental data from EC of vinasse.

Kinetic constants	Unit	7.5 V	12.5 V
k_{cg}	/s	8.06×10^{-4}	3.20×10^{-3}
α	dm^3/mol	9.02×10^{3}	10.5×10^{3}
β	J/mol	8.91×10^{1}	9.23×10^{1}
k_e	/s	5.97×10^{-5}	1.59×10^{-4}
A_f	-	2.35×10^{-4}	3.92×10^{-4}
E_f	J/mol	9.54×10^{-5}	2.01×10^{-7}
SSE	-	0.2758	0.0784

$$\frac{dV_{H_2}}{dt} = \frac{dn_{H_2}}{dt}\frac{RT}{P} = \frac{JA_eHRT}{FP} \quad (45)$$

The predicted H_2 gas is presented in Fig. 2f). From the figure, voltage 12.5 V results 1.93 dm^3 and 7.5 V results 1.01 dm^3. It causes that the scum production at 12.5 V is more than at 7.5 V. Table 3 shows the constants of A_f and E_f in which they depends on solution temperature. The frequency factor (A_f) increases and activation energy (E_f) decreases with increasing of voltage from 7.5 to 12.5 V. The less the activation energy, the easier the reaction occurs. Furthermore, the frequency factor shows the collision where the higher the frequency factor, the more often the H_2 and sludge collides to form scum. The high temperature forces the dissolved hydrogen to become H_2 gas easily. Also, it affects the big bubble size of H_2 gas. Therefore, flotation process occurs easier at 12.5 V than at 7.5 V because solution temperature at 12.5 V is higher.

Operating Cost

In EC process, the operating cost is to become one of important terms. The main components in operating cost are electrode, energy and chemical costs [4]. Furthermore, the common formula used to estimate the operating cost is shown in Eq. 46-48 [4].

$$\frac{d[Operating\ Cost]}{dt} = a\frac{d[Energy\ Cost]}{dt} + b\frac{d[Electrode\ Cost]}{dt} + c\ Chemical\ Cost \quad (46)$$

$$\frac{d[Energy\ Cost]}{dt} = \frac{VI}{v_t} \quad (47)$$

$$\frac{d[Electrode\ Cost]}{dt} = \frac{JA_eBM_{Fe}}{zFv_t} \quad (48)$$

The a is electrical energy cost with value of 30.97×10^{-5} IDR/Ws (IDR per watt second), b is iron material with value of 20 IDR/g and c is chemical cost with value of 16 IDR/g for technical grade NaOH (flake) [4]. Results of calculation for operating cost are presented in Table 4. In this study, the initial pH of vinasse is adjusted from 4.35 to 6.0. It needed amount of 8.4558 g NaOH with price of 135.29 IDR/dm^3 [4]. Furthermore electrode and energy costs needed by voltage of 12.5 V are higher than 7.5 V. Finally, the total operating cost for 7.5 and 12.5 V is 204.14 and 262.91 IDR/dm^3 respectively. Meanwhile, voltages of 7.5 and 12.5 V result the COD mass removal efficiency of 19.87 and 51.67% respectively (Table 4). Therefore, voltage of 12.5 V is more effective than 7.5 V because the former results higher ratio of COD mass removal efficiency (%) to total operating cost (IDR/dm^3) (Table 4).

Conclusion

The new kinetic model of EC is successfully developed with considering of many measured parameters which are current, pH, temperature, volume, anode weight loss, dissolved Fe concentration, COD concentration, sludge mass and scum mass. The adjustable kinetic constants in this model are k_{cg}, α, β, k_e, A_f, E_f. This model can fit the measured data of EC of vinasse at various voltages with low SSE value (0.0784-0.2758). Based on simulation, voltage of 12.5 V resulted higher k_{cg}, k_e, A_f and lower E_f values than 7.5 V.

Table 4. Operating cost of EC process in treating 1 dm^3 vinasse after 3600 sec.

Voltage	Electrode cost (IDR/dm^3)	Energy cost (IDR/dm^3)	Chemical cost [4] (IDR/dm^3)	Total operating cost (IDR/dm^3)	COD mass removal efficiency [9] (%)	Ratio of COD mass removal efficiency/ total operating cost (%/IDR/dm^3)
7.5 V	44.89	23.96	135.29	204.14	19.87	0.0973
12.5 V	83.21	44.41	135.29	262.91	51.67	0.1965

Note = COD removal efficiency = $\frac{initial\ COD\ mass\ (g) - final\ COD\ mass\ (g)}{initial\ COD\ mass\ (g)} \times 100\%$

Acknowledgement

The authors thank to Universitas Gadjah Mada via Rekognisi Tugas Akhir (RTA) Program 2020 with assignment letter of 2488/UN1.P.III/DIT-LIT/PT/2020 for financial support.

Conflict of Interest

The authors declare no potential conflict of interest regarding the publication of this work.

Nomenclatures

A_e – active surface area of electrode (dm^2)
A_f – frequency factor for flotation
A_B – base area of EC reactor (dm^2)
BM_{Fe} – molecular weight of Fe (56 g/mol)
$BM_{Fe(OH)_2}$ – molecular weight of $Fe(OH)_2$ (90 g/mol)
C_{COD} – concentration of COD (g/dm^3)
$C_{Fe(OH)_2}$ – concentration of $Fe(OH)_2$ (g/dm^3)
C_p – caloric capacity of solution (J/K)
d – distance between electrodes (dm)
E_f – activation energy for flotation (J/mol)
F – Faraday's constant (96,500 C/mol)
g – number of Hydrogen molecules per electron (½)
I – current (A)
J – current density (A/dm^2)
k_a – reaction rate constant for adsorption (/(g.s)
k_{cg} – rate constant for $Fe(OH)_2$ formation (/s)
k_e – reaction rate constant for entrapment (/s)
k_f – reaction rate constant for flotation (/s)
K_S – equilibrium constant of $Fe(OH)_2$ (mol^3/dm^9) at T
K_{s0} – equilibrium constant of $Fe(OH)_2$ (mol^3/dm^9) at T_0
K_w – equilibrium constant of water (mol^2/dm^6) at T
K_{w0} – equilibrium constant of water (mol^2/dm^6) at T_0
l_e – length of electrode (dm)
m_{anode} – weight of anode (g)
m_{COD} – mass of COD (g)
$m_{Fe(OH)_2}$ – mass of $Fe(OH)_2$ (g)
m_{scum} – mass of $scum$ (g)
m_{sludge} – mass of $sludge$ (g)
nFe_{sat} – mol of Fe^{2+} at saturation (mol)
$nFe(OH)_2$ – mol of $Fe(OH)_2$ (mol)
nFe_d – mol of total dissolved Fe^{2+} (mol)
n_{H_2} – Hydrogen amount (mol)
P – Pressure (atm)
Q – energy (J)
R – ideal gas constant (8.314 J/K.mol or 0.08206 L.atm/K.mol)
t – retention time (s)
t_e – thickness of electrode (dm)
T – solution temperature (K)
V – voltage (V)
V_{H_2} – Hydrogen volume (dm^3)
v – volume of vinasse (dm^3)
v_i – initial volume of vinasse (dm^3)
$v' - \frac{dv}{dt}$
w_e – width of electrode (dm)
x – Decrease of liquid level (dm)
z – number of electron transfer for Fe (2)
α – kinetic constant (dm^3/mol)
β – kinetic constant (J/mol)
ΔH_s – enthalpy of $Fe(OH)_2$ ionization (J/mol)
ΔH_w – enthalpy of water ionization (J/mol)
ΔT – increase in temperature (K)
$[Fe]_{sat}$ – molar of Fe^{2+} at saturation (mol/dm^3)
$[Fe^{2+}]$ – molar of Fe^{2+} (mol/dm^3)
$[H^+]$ – molar of H^+ (mol/dm^3)
$[OH^-]$ – molar of OH^- (mol/dm^3)

References

1. KERMET-SAID H., MOULAI-MOSTEFA N. Optimization of Turbidity and COD Removal from Pharmaceutical Wastewater by Electrocoagulation. Isotherm Modeling and Cost Analysis. Pol. J. Environ. Stud., **24** (3), 1049, **2015.**
2. BUI H.M. Applying Response Surface Methodology to Optimize the Treatment of Swine Slaughterhouse Wastewater by Electrocoagulation. Pol. J. Environ. Stud., **27** (5), 1975, **2018**.
3. ALI A., SHAIKH I.A., ABID T., SAMINA F., ISLAM S., KHALID A., FIRDOUS N., JAVED M.T. Reuse of Textile Wastewater After Treating with Combined Process of Chemical Coagulation and Electrocoagulation. Pol. J. Environ. Stud., **28** (4), 2565, **2019**.
4. SYAICHURROZI I., SARTO S., SEDIAWAN W.B., HIDAYAT M. Mechanistic model of electrocoagulation process for treating vinasse waste: Effect of initial pH. J. Environ. Chem. Eng. **8**, 103756, **2020**.
5. DEMIRBAS E., KOBYA M. Operating cost and treatment of metal working fluid wastewater by chemical coagulation and electrocoagulation processes. Process Saf. Environ. Prot. **105**, 79, **2017**.
6. ELAZZOUZI M., HABOUBI K.H., ELYOUBI M.S. Electrocoagulation flocculation as a low-cost process for pollutants removal from urban wastewater. Chem. Eng. Res. Des. **117**, 614, **2017**.
7. TAK B.-Y., TAK B.-S., KIM Y.-J., PARK Y.-J, YOON Y.-H., MIN G.-H. Optimization of color and COD removal from livestock wastewater by electrocoagulation process: Application of Box-Behnken design (BBD). J. Ind. Eng. Chem. **28**, 307, **2015**.
8. GARCIA-SEGURA S., EIBAND M.M.S.G., DE MELO J.V., MARTÍNEZ-HUITLE C.A. Electrocoagulation and advanced electrocoagulation processes: A general review about the fundamentals, emerging applications and its association with other technologies. J. Electroanal. Chem. **801**, 267, **2017**.
9. SYAICHURROZI I., SARTO S., SEDIAWAN W.B., HIDAYAT M. Mechanistic models of electrocoagulation kinetics of pollutant removal in vinasse waste: Effect of voltage. J. Water Process Eng. **36**, 101312, **2020**.
10. YAVUZ Y. EC and EF processes for the treatment of alcohol distillery wastewater. Sep. Purif. Technol. **53**, 135, **2007**.
11. KHANDEGAR V., SAROHA A.K. Electrocoagulation of distillery spentwash for complete organic reduction. Int. J. ChemTech Res. **5** (2), 712, **2013**.

12. ASAITHAMBI P., SAJJADI, BAHARAK, AZIZ A., RAMAN A., DAUD W., BIN W.M.A. Performance evaluation of hybrid electrocoagulation process parameters for the treatment of distillery industrial effluent. Process Saf. Environ. Prot. **104**, 406, **2016**.
13. ASAITHAMBI P., SUSREE M., SARAVANATHAMIZHAN R., MATHESWARAN M. Ozone assisted electrocoagulation for the treatment of distillery effluent. Desalination **297**, 1\, **2012**.
14. AZIZ A.R.A., ASAITHAMBI P., DAUD W.M.A.B.W. Combination of electrocoagulation with advanced oxidation processes for the treatment of distillery industrial effluent. Process Saf. Environ. Prot. **99**, 227, **2015**.
15. LU J., WANG Z., MA X., TANG Q., LI Y. Modeling of the electrocoagulation process: a study on the mass transfer of electrolysis and hydrolysis products. Chem. Eng. Sci. **165**, 165, **2017**.
16. GRAÇA N.S., RIBEIRO A.M., RODRIGUES A.E. Modeling the electrocoagulation process for the treatment of contaminated water. Chem. Eng. Sci. **197**, 379, **2019**.
17. LONE I.H. The Alternative Formulation of Van't Hoff Equation. Phys Chem Ind J **12** (2), 1, **2017**.
18. CHOU W.-L., WANG C.-T., HUANG K.-Y. Investigation of process parameters for the removal of polyvinyl alcohol from aqueous solution by iron electrocoagulation. Desalination **251**, 12, **2010**.

The New Mechanistic Model to Illustrate the Complex Phenomena in Electrocoagulation Process of Vinasse

ORIGINALITY REPORT

6%	3%	5%	%
SIMILARITY INDEX	INTERNET SOURCES	PUBLICATIONS	STUDENT PAPERS

PRIMARY SOURCES

1	Budiyono Budiyono, Iqbal Syaichurrozi, Suhirman Suhirman, Topik Hidayat, Jayanudin Jayanudin. "Experiment and Modeling to Evaluate the Effect of Total Solid on Biogas Production from the Anaerobic Co-Digestion of Tofu Liquid Waste and Rice Straw", Polish Journal of Environmental Studies, 2021 Publication	1%
2	G. Fischer, G. Karakas. "Sinking rates of particles in biogenic silica- and carbonate-dominated production systems of the Atlantic Ocean: implications for the organic carbon fluxes to the deep ocean", Copernicus GmbH, 2008 Publication	1%
3	www.gjesm.net Internet Source	<1%
4	Youn Gyeong Shin, Dan Guo, Nicholas Austin Payne, Brianna K. Rector et al. "Periodic Aggregation Patterns of Oxide Particles on	<1%

	Corroding Metal: Chemical waves due to solution feedback processes", Physical Chemistry Chemical Physics, 2022 Publication	
5	Iqbal Syaichurrozi, Sarto Sarto, Wahyudi Budi Sediawan, Muslikhin Hidayat. "Effect of Fe Addition on Anaerobic Digestion Process in Treating Vinasse: Experimental and Kinetic Studies", Periodica Polytechnica Chemical Engineering, 2023 Publication	<1 %
6	ejournal2.undip.ac.id Internet Source	<1 %
7	illnesshacker.com Internet Source	<1 %
8	Sincero, . "Coagulation", Physical-Chemical Treatment of Water and Wastewater, 2002. Publication	<1 %
9	repository.publisso.de Internet Source	<1 %
10	www.degruyter.com Internet Source	<1 %
11	Andi Dharmawan, Lazuardi Ichsan, Hanif Baskoro, Jazi Eko Istiyanto, Ariesta Martiningtyas Handayani. "Attitude and Horizontal Speed Control System on Unmanned Aerial Vehicle Using LQR", 2019	<1 %

5th International Conference on Science and Technology (ICST), 2019
Publication

---

12 Chusni Ansori, Puguh Dwi Raharjo, Agung Setianto, I Wayan Warmada, Nugroho Imam Setiawan. "Geomorphology and iron sand potential at coastal sediment morphology, Kebumen Regency", E3S Web of Conferences, 2020 <1%
Publication

---

13 Hakizimana, Jean Nepo, Bouchaib Gourich, Mohammed Chafi, Youssef Stiriba, Christophe Vial, Patrick Drogui, and Jamal Naja. "Electrocoagulation process in water treatment: A review of electrocoagulation modeling approaches", Desalination, 2017. <1%
Publication

---

14 ndl.ethernet.edu.et <1%
Internet Source

---

15 M. Favre, D. Landolt, K. Hoffman, M. Stratmann. "Influence of gallic acid on the phase transformation in iron oxide layers below organic coatings studied with Moessbauer spectroscopy", Corrosion Science, 1998 <1%
Publication

---

16 Saumya Agrawal, Tabish Nawaz. "Produced Water Treatment By Electrocoagulation <1%

Process: Experimental and Modelling Study", American Chemical Society (ACS), 2022
Publication

17 C Vallois. "Separation of H+/Cu2+ cations by electrodialysis using modified proton conducting membranes", Journal of Membrane Science, 2003 <1%
Publication

18 Hana Měšťánková, Gilles Mailhot, Jaromír Jirkovský, Josef Krýsa, Michèle Bolte. "Effect of iron speciation on the photodegradation of Monuron in combined photocatalytic systems with immobilized or suspended TiO2", Environmental Chemistry Letters, 2008 <1%
Publication

19 Tamura, H.. "The role of rusts in corrosion and corrosion protection of iron and steel", Corrosion Science, 200807 <1%
Publication

Exclude quotes	On	Exclude matches	Off
Exclude bibliography	On		

The New Mechanistic Model to Illustrate the Complex Phenomena in Electrocoagulation Process of Vinasse

GRADEMARK REPORT

FINAL GRADE

/0

GENERAL COMMENTS

Instructor

PAGE 1

PAGE 2

PAGE 3

PAGE 4

PAGE 5

PAGE 6

PAGE 7

PAGE 8

PAGE 9

PAGE 10

PAGE 11